applied sciences

MDPI

Article

The Shear Strength of Granite Weathered Soil Under Different Hydraulic Paths

Youqian Lu [1,2,*], Guoqing Cai [1,2,*] and Chenggang Zhao [1,2]

1 Key Laboratory of Urban Underground Engineering of Ministry of Education, Beijing Jiaotong University, Beijing 100044, China; cgzhao@bjtu.edu.cn
2 School of Civil Engineering, Beijing Jiaotong University, Beijing 100044, China
* Correspondence: luyouqian@bjtu.edu.cn (Y.L.); guoqing.cai@bjtu.edu.cn (G.C.)

Received: 13 August 2020; Accepted: 18 September 2020; Published: 22 September 2020

Abstract: At present, there is no clear understanding of the influence of differences in soil mineral composition, particle size grading, and hydraulic paths on the shear strength of unsaturated soil, and the related strength models are not applicable. The shear strength characteristics of different saturation specimens under different hydraulic paths were studied on two granite weathered soils. The experimental results show that the shear strength index of the prepared specimen is "arched" with the increase of saturation, and the dehydration specimen decreases linearly with the saturation. As considering the cementation of free oxides in soils and the interaction among soil particles at different saturations, it is assumed that there are three different contact modes among soil particles: direct contact, meniscus contact, and cement contact. The difference in contact modes will reflect the different laws of shear strength. A shear strength model capable of distinguishing between the capillary effect and the adsorptive effect was established. The model predicted and verified the shear strength data of granite weathered soil under different hydraulic paths well, and then theoretically explained the evolution law of the shear strength of granite weathering soil under the change of saturation.

Keywords: weathered granite soils; shear strength; saturation; capillary effect; adsorptive effect

1. Introduction

Shear strength is the ultimate ability of soil to resist shear force, which is one of the most important indexes of soil mechanical properties. The pressure of retaining wall, bearing capacity of foundation, and stability of landslide and collapse in a natural environment are all related to the shear strength of the soil. Soils in unsaturated states are much more commonly seen in nature [1–3]. The shear strength of unsaturated soils depends on several factors such as soil type, particle distribution, density, hydraulic path, and stress state [3–5].

Over the past few decades, a number of laboratory tests have been conducted to study the hydraulic behavior of unsaturated soils in the low suction range using axial translation techniques [6–9]. The suction was less than 500 kPa in most direct shear or triaxial tests, and the test soil was mainly sand or silt. However, in geotechnical engineering, unsaturated soils with high or wide suction range are widespread, and soil types contain a lot of silty clay or clay. At the same time, it is challenging to control suction in mechanical tests in high suction range accurately, and the vapor flow technique or the osmotic suction techniques have been adopted to control the high suction of specimens [10–13]. However, the test results of unsaturated soil mechanical behavior under high suction in the literature are still intensely limited. In addition, most existing shear strength models are based on analysis of test results obtained by direct shear or triaxial shear tests at low suction ranges (typically below 500 kPa). As a result, the shear strength of unsaturated soils in the medium suction range is significantly overestimated,

especially for clays [14,15]. Through the verification and comparison of various existing strength models, it is found that most of them are based on an empirical and phenomenological basis, and there are few explanations and simulations for the strength in the medium and high suction range [14]. On the other hand, different soil types, such as sand and clay, exhibit differences in microscopic states, which often significantly affect the strength of the soil. Soils in nature are complex and vary widely in their microscopic structure and mineral composition [16]. Although there are numerous models, there is no widely accepted method for strength influence mechanism and model calculation. Therefore, it is necessary to study the influence mechanism of different soil types, particle distribution, hydraulic path, and stress state on soil strength under high suction or wide suction range and establish a corresponding strength model.

The widely distributed granite weathered soil is affected by its soil-forming environment and geotechnical composition [17,18]. Its physical and mechanical properties are unique, especially the microstructure of its profile variation [19,20], which also causes difficulties in numerical simulation of the mechanical behavior and engineering characteristics of weathered granite soil. Therefore, the granite weathered soil can be used as a typical research object in the study of unsaturated strength. There is an urgent need to clarify the mechanism of action of various factors that affect the strength of granite weathered soil, and establish a model directly used to simulate or explain its physical and mechanical characteristics under a wide suction range. Therefore, in this paper, the direct shear strength test of two different weathered granite soils under different hydraulic paths is carried out, and the evolution law of the soil strength on the effect of mineral composition and particle size gradation is analyzed under a wide suction range. The factors affecting the strength change of granite weathered soil are explained by the contact modes between soil particles established, and further verified and explained by scanning electron microscope (SEM) from the perspective of microscopic mechanism. The relationship between soil suction and strength is also discussed, and a shear strength model that is applicable and has a clear physical concept is established.

2. Materials and Methods

2.1. Physical and Chemical Properties of Weathered Granite Soil

The test soil was taken from a typical granite weathered soil in a slope in Wuzhou in Guangxi Autonomous Region, China. According to the weathering profile and erosion characteristics, the soil was divided into the residual soil layer and the fully weathered soil layer [21]. Representative samples were taken from the residual soil zone (2–5 m from the ground surface) and the fully weathered soil zone (6–10 m from the ground surface). As shown in Figure 1, the residual soil is brick red or brownish red with a small amount of white quartz particles; the fully weathered soil is mainly yellow-brown, mixed with red and white. Figure 2 indicates the measured particle gradation curve of the two soils. The content of residual soil with particle size less than 0.002 mm reaches 22%, while only about 5% in fully weathered soil and more than 50% of fully weathered soil is sand. The feature of grading curve of the granite weathered soils used in this paper is consistent with the typical granite weathering characteristics [18,21]. According to the soil particle size and structural characteristics, and the classification of granite weathered soils [22], the residual soil and the fully weathered soil adopted in this paper are named silty clay and silty sand, respectively.

The basic physical and chemical indexes of the two soils are shown in Tables 1 and 2. The main minerals such as potassium feldspar, plagioclase, and mica of granite are enriched by weathering, hydrolyzed and oxidized to form secondary silicates such as kaolinite and illite. Because granite weathering is a process of enriching iron and aluminum, iron oxide and alumina remain, which could be hydrated to form cementation. X-ray diffraction(XRD) quantitative test results of clay minerals show that weathered granite is mainly composed of elo and illite, accompanied by quartz and calcium carbonate [23]. The degree of weathering makes the difference in the content of weathered products

distinct, resulting in the specific gravity, liquid-plastic limit, and specific surface area of residual soil being significantly higher than that of fully weathered soil.

(**a**) (**b**) (**c**) (**d**)

Figure 1. Sample of weathered granite soils: (**a**) powder of fully weathered soil; (**b**) powder of residual soil; (**c**) sample of fully weathered soil; and (**d**) sample of residual soil.

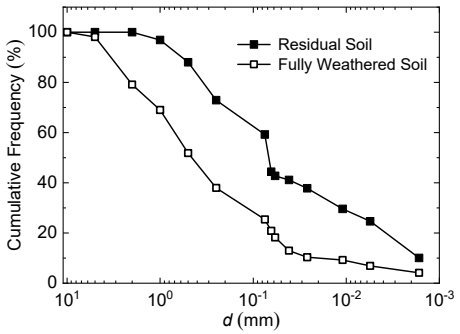

Figure 2. Grading curve of weathered granite soil.

Table 1. Physico-chemical property of granite weathered soil.

Property \ Sample	Residual Soil	Fully Weathered Soil
Liquid limit	55.8%	43.7%
Plastic limit	30.3%	28.6%
Plasticity index	24.5%	15.1%
Specific gravity	2.71	2.66
Specific surface area (m^2/g)	107.2	70.2
Cation exchange capacity (meq/100 g)	29.5	21.2

Table 2. Fully chemistry analysis of silicate.

Project \ Sample	Residual Soil	Fully Weathered Soil
SiO_2	69.83	68.28
Al_2O_3	16.91	16.36
Fe_2O_3	4.58	3.07
FeO	0.19	1.14
K_2O	1.45	4.31
Na_2O	0.056	0.23
CaO	0.017	0.032
MgO	0.17	0.65
Loss on ignition	6.57	4.97

2.2. Direct Shear Test and The Soil–Water Characteristic Curve Test of Weathered Granite Soil

The test soil was dried and sieved through a 2-mm screen, and the dry density of the specimen took the average value of the two samples, namely 1.55 g/cm^3. The test uses a ZJ-2 strain control type direct shear instrument, and the specimens were sheared under unconsolidated-undrained with the vertical pressures of 100, 200, 300, and 400 kPa (shearing rate is 0.8 mm/min). The method of soil–water characteristic curve test is reference [23]. All the tests were performed at room temperature of about 20 °C.

Hydraulic path 1 (Prepared specimen referred to as P): Prepare specimens with initial saturation of 20, 40, 60, and 80% respectively. Specifically, it is to prepare soils with different initial moisture content corresponding to the target saturation, after sealing and moisturizing for h, weigh the soils of corresponding quality to make the specimens by static compact method, the error of saturation is controlled within ±0.5%. The 100% saturated specimen is obtained by pumping and saturating the specimen with an initial saturation of 20% and then the direct shear test is carried out after standing for 24 h.

Hydraulic path 2 (dehydrated specimen referred to as D): The saturated sample is dehydrated slowly in a constant temperature and humidity box with a relative humidity of 25% and a temperature of 20 °C to achieve 20, 40, 60, and 80% saturation. The water content of the specimen is controlled by the mass weighing method, and the specimen body change is measured by the shrinkage instrument and vernier caliper method. The error of saturation is controlled within ± 0.5%. After reaching the corresponding saturation, the specimen is taken out for direct shear test (the body changes little during the dehydration process, so ignore the influence of body changes).

2.3. Simulation of Existing Strength Model

At present, the shear strength equations are established based on Bishop's effective stress [24] or independent stress variables (mean net stress and matric suction) [25]. Alonso et al. [26] compared and commented on the selection of stress state variables for unsaturated soils, they considered that the two stress variable forms of Bishop stress (effective stress) and suction should be uncontested choices as Equation (1). The main difference between many strength equations is the difference in the adsorption strength as Equation (2), and the setting of the parameter of χ in the strength equation in the Bishop format, which is mainly a function of saturation [14,27]. In order to verify the applicability of the model to the experimental results of weathered granite soils, the corresponding suction value of the corresponding saturation was obtained by using the soil–water characteristic curve, and the strength was calculated by Bishop shear strength equation of $\chi = S_r$

$$\tau_f = c' + (\sigma - u_a)\tan\varphi' + \chi(u_a - u_w)\tan\varphi' \quad (1)$$

$$c = \chi(u_a - u_w)\tan\varphi' \quad (2)$$

where τ_f is the shear strength, c is the adsorption strength, c' is the effective saturation cohesion and φ' is effective internal friction angle, χ is effective stress parameter, $u_a - u_w$ is net normal stress, and $u_a - u_w$ is matric suction.

3. Results

3.1. Results of the Direct Shear Test and the Soil–Water Characteristic Curve Test

Under different saturation and stress states, the failure mechanism of the specimen is different. When the saturation is low, the specimen is brittlely broken, and the peak and residual strength of the direct shear strength appear; at high saturation, the specimen may undergo plastic failure, that is, with increasing shear displacement, the strength will continue to increase without peak strength. Therefore, the shear strength of specimen is determined as follows: for brittle failure, the strength value is taken as its peak strength, and for plastic failure, the strength value is taken when the shear

displacement is 4-mm. The strength failure line is shown in Figure 3. It is known from Figure 3 that the corresponding intensity values of residual soil at different initial saturations are significantly higher than that of fully weathered soils. The strength of the prepared specimens of both soils increased first and then decreased with saturation increased, and the peak intensity appears at S_r = 40%. At the same time, dehydrated specimens present different trends. As the saturation decreases, the shear strength of the specimen will continue to increase. The dehydrated sample with the same saturation has a higher shear strength value than the prepared sample; The opposite trend even occurs at low saturation, the strength of the prepared sample is relatively low and that of the dehydrated sample is the highest when S_r = 20%.

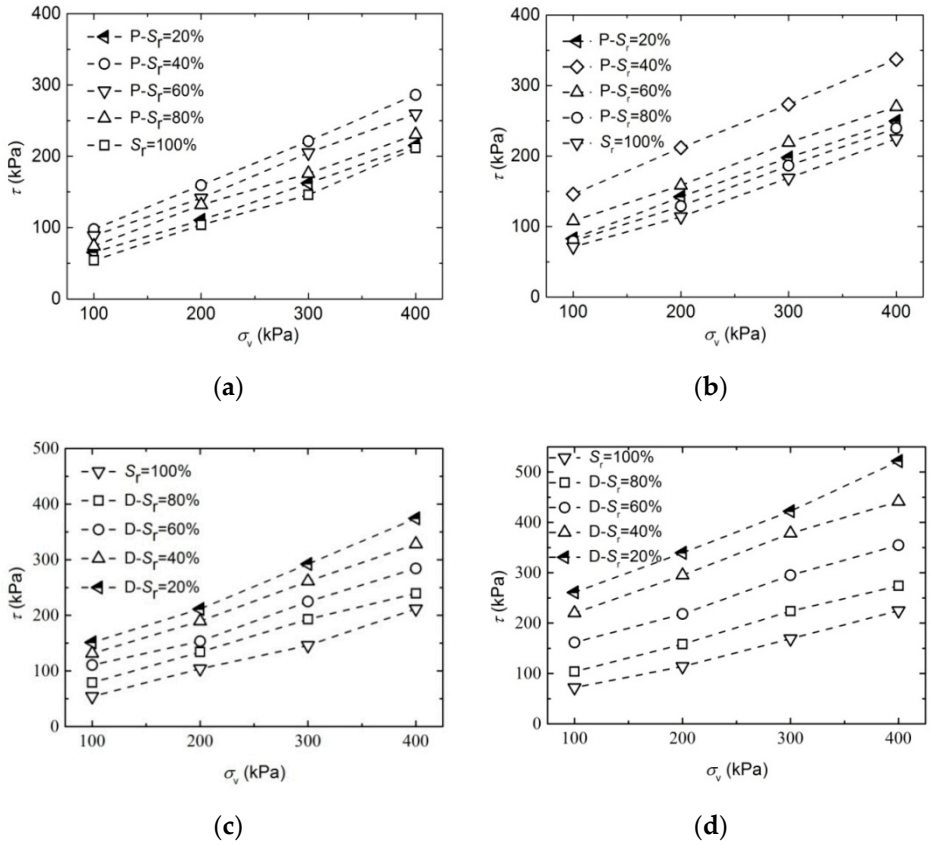

Figure 3. Relationship between shear strength and vertical pressure of samples with different saturation: (**a**) Preparation sample of fully weathered soil; (**b**) Preparation sample of residual soil; (**c**) Dehydrated sample of fully weathered soil; and (**d**) Dehydrated sample of residual soil.

Figure 4 indicates the change of cohesive force and internal friction angle with saturation of the granite weathered soil. From Figure 4, we can see that the changing trend of the cohesive force and friction angle of the specimen is consistent with the changing trend of the strength value of the hydraulic path. However, the friction angle of the prepared specimen does not change much. The changing range of the prepared specimen is within 5°, and the change amplitude of the dehydrated specimen does not exceed 10°. When $S_r \leq 60\%$, the friction angle of the dehydrated specimen of fully weathered is greater than that of residual soil, which is related to the fact that fully weathered soil contains more sand. As can be seen from Figure 4b, the cohesion of both soils is more sensitive to saturation, while the residual soil changes more drastically; when S_r = 100%, the cohesion of fully weathered soil is 5 kPa, the amplitude of its prepared specimen is still small. However, the dehumidification specimen increases linearly with the decrease of saturation, reaching 98 kPa when S_r = 20%. The cohesion of the residual soil changes obviously whether it is prepared specimens or dehydrated specimens, the peak value of the prepared specimens has reached 81 kPa, and the linear change rate of the dehydrated

specimens is also more significant than that of the fully weathered soil. This is related to the residual clay containing more clay particles, iron oxide, and other types of cementation, which will be analyzed in detail below.

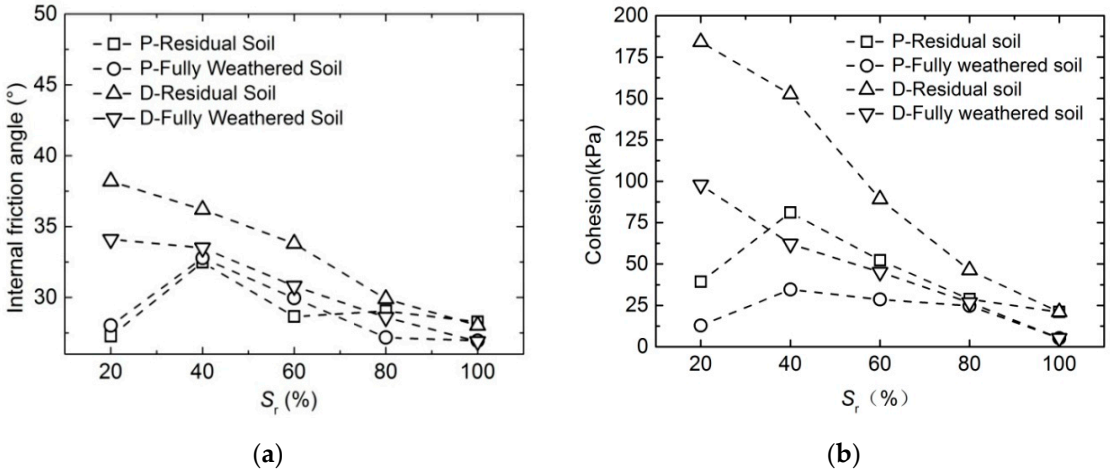

(**a**) (**b**)

Figure 4. Relationship between cohesion and saturation curve: (**a**) Relationship between internal friction angle and saturation; (**b**) Relationship between cohesion and saturation curve.

Figure 5 is the soil–water characteristic curve (SWCC) of the whole range of suction of the granite weathered soil obtained by the pressure plate method and the salt solution method [23]. The soil–water characteristic curve is a functional curve describing the constitutive relation between soil suction and water content (saturation), which is often used to calculate the strength of the soil [1]. The residual soil has higher water holding capacity than the fully weathered soil, the detail of comparison and analysis can be seen [23].

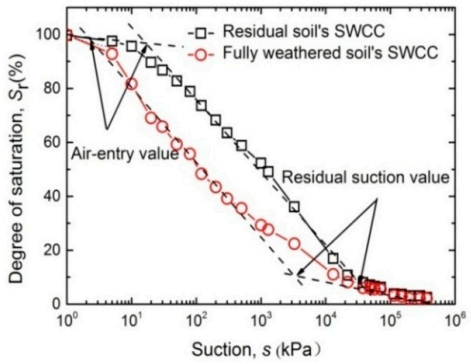

Figure 5. Soil–water characteristic curve of weathered granite soil.

3.2. Simulation Results of Existing Strenth Model

The experimental results and calculated values are shown in Figure 6. At low suction, the deviation between the experimental results and the predicted value is small, while at high suction, the deviation is massive, especially for dehydrated residual soil. This is consistent with Alonso et al.'s belief that the strength equation in the form of Bishop and Fredlund will be significantly large in the high suction section. This is consistent with Alonso et al.'s view [26] that the strength equation of Bishop and Fredlund will appear to be severely large in the high suction section. On the other hand, at high suction, the strength of the prepared specimen does not increase with the increase of suction. On the contrary, there is a decrease in strength, but the strength equation does not reflect it. Although the suction value used in the calculation is the soil–water characteristic curve of the dehydrated sample and not the actual curve of the prepared sample, there is a certain deviation in the suction value, which does not

affect the regular trend in Figure 6. Therefore, this type of equation is not suitable for the calculation of the shear strength of granite weathered soil containing cementation. It is necessary to establish a new model to simulate such soils as weathered granite soil.

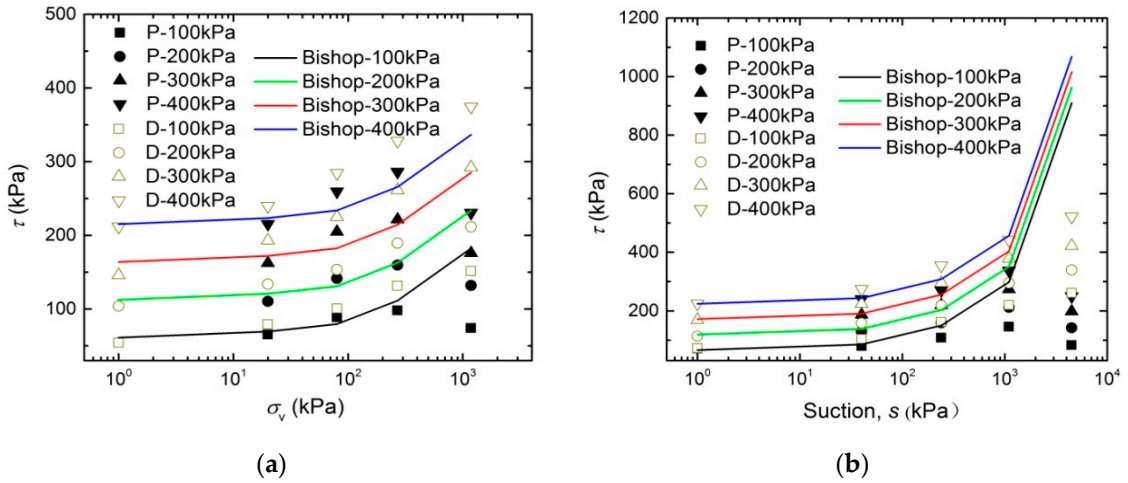

Figure 6. Relationship between suction and strength of weathered granite soil: (**a**) fully weathered soil; (**b**) residual soil.

4. Discussion

4.1. Effect of Particle Size Gradation and Mineral Composition on Shear Strength

According to the interaction of soil particles in different mineral compositions and water holding states, it is assumed that there are three different forms of contact between particles in the soil as shown in Figure 7: Figure 7a displays that when the saturation is high, the pores are filled with water, and a small amount of meniscus mainly provides the shear strength. When the saturation is low, as shown in Figure 7b, there are three modes of inter-particle contact: (1.) The soil particles are in direct contact with the adsorbed water film, due to the relative largely density, the adsorbed water cannot flow, which can be regarded as a solid or semi-solid [28]. (2.) There is a meniscus contact by the capillary between the soil particles. (3.) The cement contact in which solidified cementation materials bind soil particles tightly together.

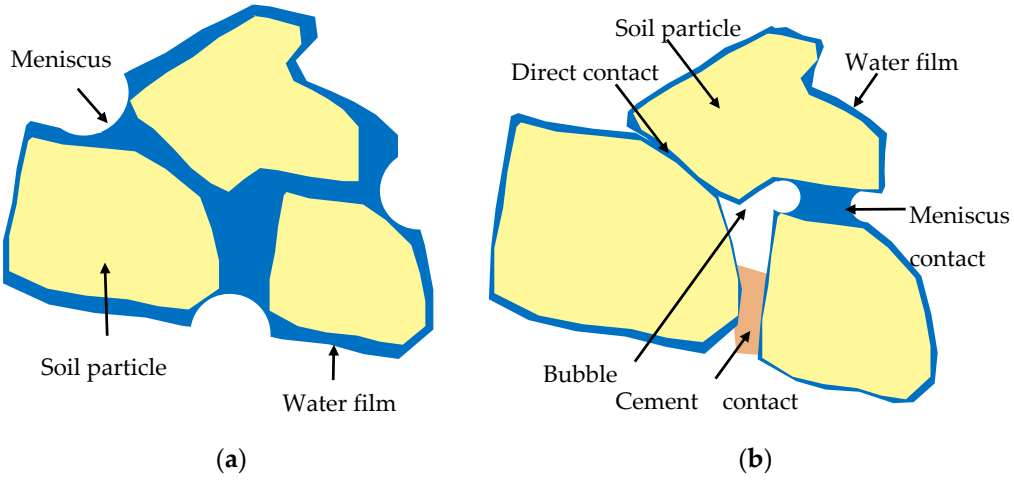

Figure 7. Soil particle contact model: (**a**) Saturated state; (**b**) Unsaturated state.

(1) When there is no cementation substance and the saturation is low, the contact types between the soil particles are mainly direct contact and meniscus contact. The content of the capillary

meniscus increases first and then decreases as the saturation increases. The optimal saturation occurs when there is the largest soil–water contact area in the soil, with the most meniscus contact, thereby increasing the shear strength of the soil. On the other hand, the pore size and distribution in the soil body will affect the characteristics of the meniscus, while the particle size of the soil particles and the mineral composition affect the pore size and distribution of the soil [23]. According to the Young–Laplace equation, small pores have a more substantial capillary effect than large pores [29]. Therefore, the particle size gradation and the mineral composition in the soil control the contact form and relative content of the soil particles, as well as their intensity of action, which in turn affects the law of shear strength.

(2) When there are cementation materials in the pore fluid, the cement contact forms between soil particles in addition to direct contact and meniscus contact. Part of the iron oxide in the soil will be distributed on the whole or part of the surface of the clay particles in the form of "envelope", and it will be cemented together in the form of "bridge" to increase the strength of the soil, and the other part will exist as free iron oxide. The key to the "envelope" formation lies in the saturation of the soil and the content of free iron oxide. With low saturation, the solid particles of iron oxide in the soil cannot be dissolved in the pore fluid to form a sol; with high saturation, the water film between the soil particles is so thick that it cannot create cementation but exists in a free state. The free iron oxide will gradually develop a colloidal "envelope" as the saturation decreases from the wet state to the dry state. It is known from Table 1 that the more severely weathered residual soil contains higher residual Fe_2O_3, Al_2O_3, and organic matter than the fully weathered soil (other oxides cannot be dissolved to form free oxides), which makes the residual soil contain more cementation. On the other hand, the larger specific surface area and cation exchange capacity of the residual soil can make the soil particles adsorb more ions and increase the soluble salt in the pore fluid, which can produce the same cementation effect as free iron oxide [30]. The cementation makes the shear strength of the residual soil higher than that of the fully weathered soil and makes the shear strength of the dehydrated specimen higher than that of the prepared sample.

Figure 8 is a 2000-times scanning electron micrograph of the prepared specimens and dehydrated specimens of granite weathered soil when S_r = 20%. It is known from Figure 8 that the content of coarse particles (blocks or flakes with smooth surface in the picture) in fully weathered soil is relatively high, and the skeleton of the soil body is mainly composed of coarse particles. The clay particles are filled in the large pores of the coarse particles with a floc structure (the surface looks rough and the volume is large or small) to control the micropore structure; The residual soil has a high content of clay particles, and the soil skeleton is mainly composed of floc structure and has more micropore structure, with some cracks or large pores interspersed. Therefore, at low saturation, the residual soil contains more meniscus than the fully weathered soil. On the contrary, the fully weathered soil contains more direct contact. Macroscopically, it has a larger friction angle. The residual soil has greater cohesion due to more meniscus contact and cement contact. It is known from Figure 8a,b that the fully weathered soil contains more flaky and coarse particles, and the particle pores of the dehydrated sample contain more floc structure than the prepared sample. It is also known from Figure 8c,d that the flocculation structure of the dehydrated sample of residual soil is more compact and uniform than that of the prepared sample; that is, the dehydrated sample forms more cement contacts. Therefore, the structural composition and mineral composition of the soil determine the contact form between the particles, and the dominant contact form under different hydraulic paths determines the law of the shear strength. At the same time, these factors also affect the water-holding characteristics of the soil. In unsaturated soil mechanics, suction is usually used as a representative variable, and the influence of suction on strength will be quantitatively studied in the following part.

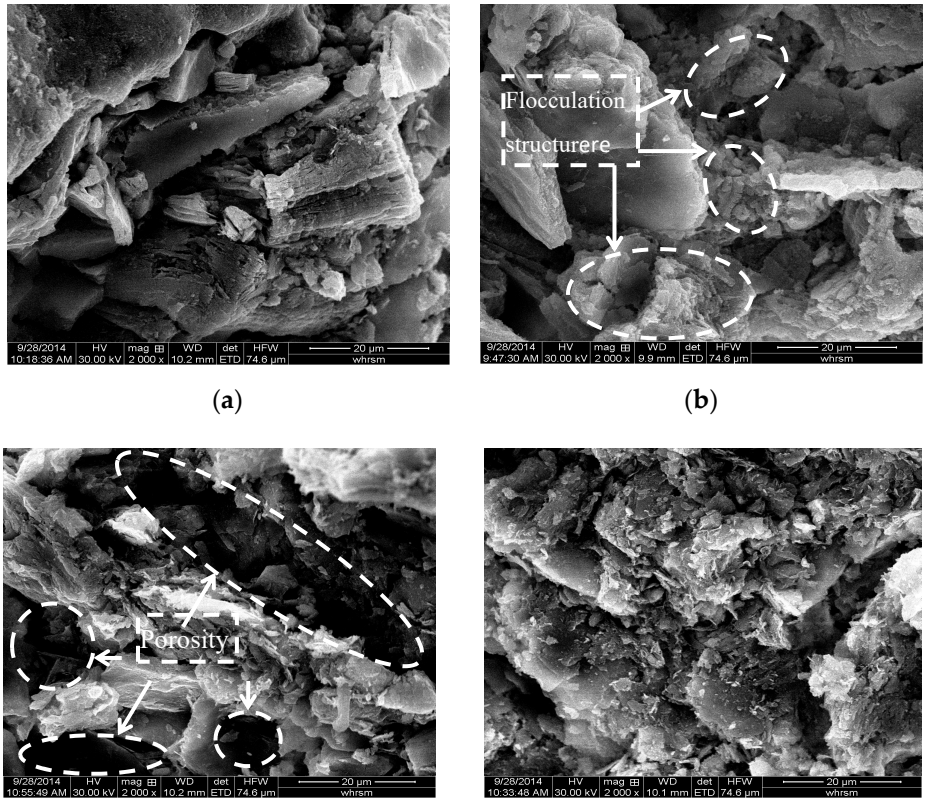

Figure 8. Scanning electron microscope (SEM) of granite weathered soils: (**a**) Preparation sample of fully weathered soil; (**b**) Dehydrated sample of fully weathered soil; (**c**) Preparation sample of residual soil; and (**d**) Dehydrated sample of residual soil.

4.2. Effect of Suction on Shear Strength and Model Establishment

At present, the mechanism of matric suction on strength is mainly aimed at capillary pressure caused by surface tension. According to the microcosmic study of soil particle contact model above, the matric suction not only includes the suction generated by the capillary phenomenon, but also includes capillary and adsorptive suction. Other scholars also hold unanimous views [31,32]. The adsorptive part is a complex interaction between soil and water, including short-range van der Waals forces, long-range electrostatic forces, and other hydration, namely physico-chemical interactions [16,33]. Cement contact caused by cementation substances such as free oxides, soluble salts, and organic matter is a typical part of adsorptive suction. At high saturation, the adsorptive part also occupies a large proportion; at low saturation, the capillary effect is no longer effective, and the dominant is the clay mineral and the soil–water interaction that adsorbs water [25,31]. In the existing unsaturated strength equation [14,26], the effect of capillary and suction on strength is confused, and the mechanism of capillary action is relatively clear, and the mathematical treatment is relatively simple. Therefore, in the quantitative research of unsaturated soil mechanics, matric suction is often equated with the capillary part and the adsorptive part is ignored. The constitutive models established for unsaturated soils are mostly based on the capillary mechanism, so these models are not suitable for high plastic clays, soils containing cementation, or low water content.

According to the previous micro research and the existing problems in the current model, this paper divides the shear strength of soil into capillary and adsorptive parts as shown in Equation (3). Konrad and Lebeau [34] used the capillary model to clarify the relationship between the capillary strength generated by the capillary water and the matric suction. A capillary model of a typical silty soil was obtained, and the capillary strength was first increased and then decreased with the matric

suction. Referring to the ideal capillary model of silt, the strength is shown in Equation (4) when only the capillary effect is considered, and the adsorptive effect is ignored. According to Equation (4), the relationship between soil strength and matric suction is shown in Figure 9. The shear strength of soil increases first and then decreases with the increase of matric suction

$$\tau_f = \tau_f^{cap} + \tau_f^{ads} \tag{3}$$

$$\tau_f^{cap} = c' + \left[\overline{\sigma}_n + s\left(\frac{S_r - S_{r,r}}{1 - S_{r,r}}\right)^{\frac{0.55}{\lambda}}\right]\tan\varphi' \tag{4}$$

where τ_f is the total shear strength, τ_f^{cap} is the shear strength of the capillary effect, τ_f^{ads} is the shear strength of the adsorptive effect, $\overline{\sigma}_n$ is net stress, $S_{r,r}$ is residual saturation, S_r is total saturation, and λ is the parameter fitted according to the experimental data.

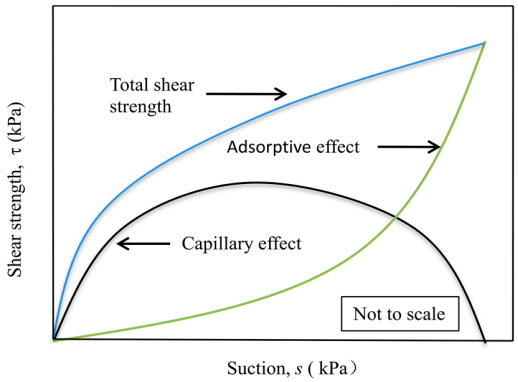

Figure 9. Relationship between shear strength and matric suction.

For special soils, such as granite weathered soil containing cementation, the contact form between the soil particles under the dehumidification path includes not only meniscus contact, but also cement contact. Equation (4) is for soils dominated by capillary models such as low plastic silty soil or sandy soil, so it is necessary to introduce the influence of adsorptive suction. Tang et al. [35] believed that the adsorptive part is mainly a variable structure suction that changes with saturation. The variable structure suction includes the cementation between the soil particles, the electric double layer suction, the bite force, and the physical–chemical force and other forces. Therefore, the strength of the adsorptive part is generally expressed as a function of the strength of the cementation. It gradually increases as the saturation decreases, and the growth rate will vary with soil properties. Kong et al. [36] summarized the cementation function as Equation (6) based on a large number of test data on the influence of saturation on soil strength. Figure 10 indicates the characteristic curves of the cementation function under different parameters. From Figure 10, it can be seen that the cementation function curve can be either a concave function or a convex function, which can simulate different growth laws of cementation strength. The effect of the cementation strength of structural soil is related to stress [37], and considering the degradation model of the cementation strength function under the condition of no stress, the cementation strength derived in this paper is shown as Equation (5). The overall strength equation is shown as Equation (7), which is the sum of the capillary effect and adsorptive effect.

$$\tau_f^{ads} = (\overline{\sigma}_n + s_0)C(S_r) \tag{5}$$

$$C(S_r) = a(1 - S_r^b) \tag{6}$$

$$\tau_f = c' + \overline{\sigma}_n \tan\varphi' + \left(\frac{S_r - S_{r,r}}{1 - S_{r,r}}\right)^{\frac{0.55}{\lambda}} s\tan\varphi' + (\overline{\sigma}_n + s_0)a(1 - S_r^b) \tag{7}$$

in the equation, $C(S_r)$ is the cementation strength function related to saturation, s_0 is the intake value, and a,b are the fitted parameters according to the test data.

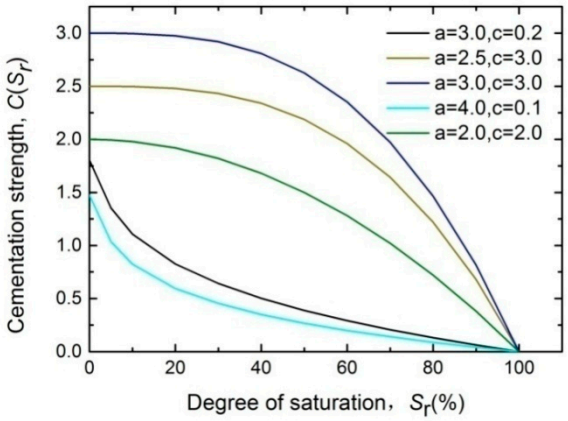

Figure 10. Cementation function characteristic curve.

Figure 9 is a simulation curve of the relationship between suction and strength in soil, clarifying the contribution and mechanism of capillary and adsorptive effects on strength. The soil strength is considered as an ideal capillary model when the viscosity absorption strength caused by cementation substances such as clay content, free iron oxide, and organic matter is ignored; that is, the contribution of capillary action to the strength is considered only. As shown in Figure 9, the strength of the soil increases first with the increase of saturation, and there is an optimal saturation to achieve the maximum strength of the soil. Then, as the saturation increases, the strength of the soil begins to decrease, and the variation law of the shear strength of the prepared specimen of weathered granite soil is like this. When there is cementation material in the pore solution, as the saturation decreases, the cementation material dissolved in the pore fluid continuously precipitates to increase the cementation strength of the soil, which explains the law of the shear strength of the dehydrated specimen of granite weathered soil well. For simplification, considering that the adsorptive of the prepared specimen contributes little to the strength of the soil, so only the capillary effect is considered during the calculation of the model. Since only the soil–water characteristic curve test results of the dehydrated soil samples are available, the capillary action in the dehydrated samples will be assumed to be consistent with that of the prepared samples in the calculation. Figure 11 indicates the comparison between the experimental results of the shear strength of granite weathered soil and the simulation results of Equation (7), and Table 3 presents the relevant parameters calculated by the model.

Table 3. Basic parameters of the model.

Parameter \ Sample	Residual Soil	Fully Weathered Soil
c' (kPa)	20.98	5.22
φ (°)	28.25	26.9
$S_{r,r}$ (%)	16	18
λ	0.35	0.65
a	4.5	2
b	0.1	0.14

As can be seen from Figure 11, this model has a high degree of fitting to the test results, indicating the correctness and validity of the model. The calculation after the simplified model assumption has a high degree of fit. Still, it is worth noting that: the soil–water characteristic curve used in the model calculation is the soil–water characteristic curve of the dehydrated specimen, and the

prepared specimens with different initial water content will produce different pore size distributions, which makes the simulated strength of medium and high suction lower than the actual test strength. The strength simulation of the dehydrated specimen directly uses the capillary effect parameters of the prepared specimen, which is one of the reasons that the simulation results are low when its suction is high. On the other hand, although there may be some changes in the saturation and suction of the specimen during the direct shear test, there is a certain deviation that cannot accurately describe the strength characteristics of unsaturated soil under the three-dimensional stress state. However, the direct shear test can accurately and simply reflect the strength characteristics of soil under different hydraulic paths to a certain extent, which provides a valid test basis for the establishment of the model.

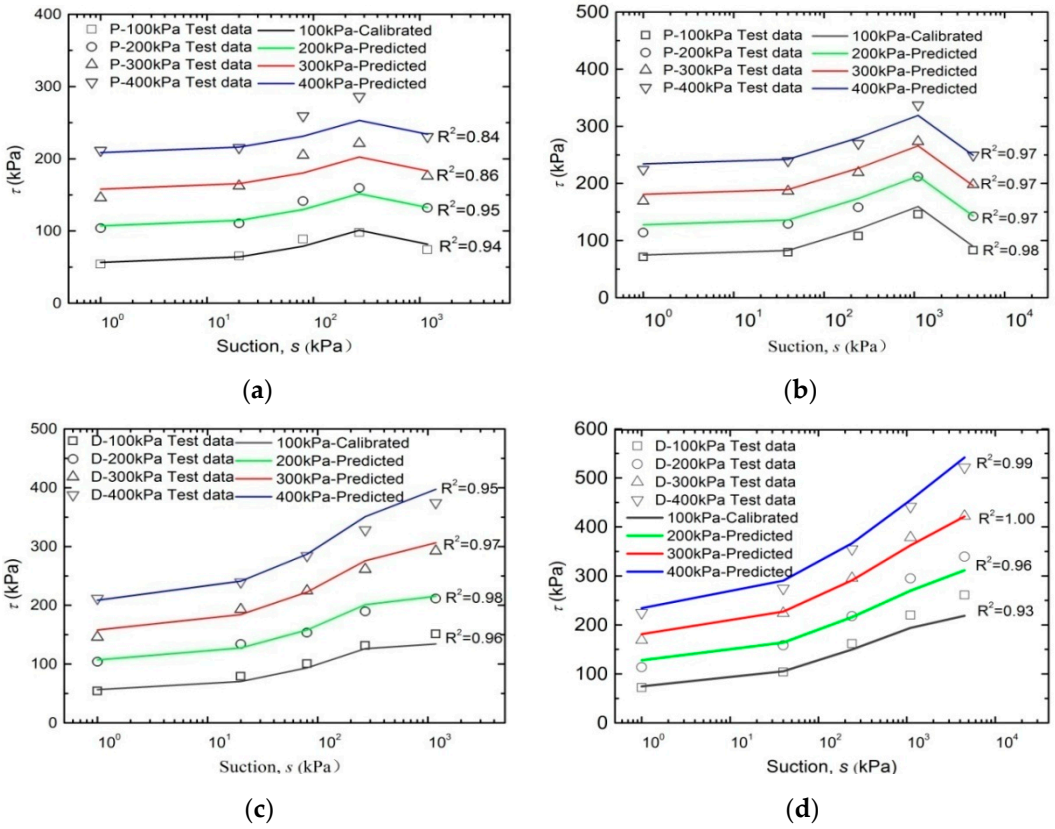

Figure 11. Comparison of experimental and simulated results of shear strength of weathered granite soil: (**a**) Preparation sample of fully weathered soil; (**b**) Dehydrated sample of fully weathered soil; (**c**) Preparation sample of residual soil; and (**d**) Dehydrated sample of residual soil.

5. Conclusions

In this paper, the shear strength test of two weathered granite soils with different saturations under the influence of different hydraulic paths is carried out. The effect of mineral composition and particle size gradation on shear strength are further discussed, and a shear strength model of unsaturated soil considering capillary and adsorption effect is established. The main conclusions are as follows:

(1) The shear strength of the prepared specimen increases first and then decreases with the increase of saturation. It reaches the peak strength at the optimal saturation S_r = 40%, showing an "arch" change. The shear strength of the dehydrated specimen increases linearly with the decrease of saturation. The cohesion of weathered granite soil varies significantly with saturation, while the amplitude of the internal friction angle with saturation varies little.

(2) There are three different contact forms: direct contact, meniscus contact, and cement contact between soil particles. Different granite weathering degree makes the residual soil and fully weathered soil different in particle size gradation and mineral composition, the contact

form between the soil particles is jointly determined under the effect of the hydraulic path, which ultimately affects the strength characteristics of the soil under different saturations.

(3) A strength model which can consider both the capillarity and adsorptive effect is established, which can thoroughly explain the action mechanism and influence law of capillarity and adsorptive on soil strength, and well explain and simulate the evolution law of shear strength of granite weathering soils with different saturation under different hydraulic paths. According to the deficiencies of the existing strength model, this model provides a clear theoretical basis for the strength research of special soils such as weathered granite soil, and it is easy to generalize and apply to other simple soil types in unsaturated soils. The prediction and verification of other soils will be improved in the next step.

Author Contributions: Y.L. and G.C. designed and performed the experiments, analyzed the data, and wrote the paper. Y.L., G.C., and C.Z. cooperated with the data analysis and manuscript elaboration. All authors have read and agreed to the published version of the manuscript.

Funding: This work was supported by the Fundamental Research Funds for the Central Universities (2020CZ002, 2020JBM048), the National Natural Science Foundation of China (51722802, 51678041, and U1834206), the Natural Science Foundation of Beijing Municipality (8202038), and Beijing Nova Program (Z181100006218005).

Conflicts of Interest: The authors declare no conflict of interest.

References

1. Fredlund, D.G.; Rahardjo, H. *Soil Mechanics for Unsaturated Soils*; Wiley: New York, NY, USA, 1993.
2. Vanapalli, S.K. Shear Strength of Unsaturated Soils and Its Applications in Geotechnical Engineering Practice. In Proceedings of the 4th Asia Pacific Conference on Unsaturated Soils, Newcastle, Australia, 23–25 November 2009; Taylor & Francis Group: London, UK, 2010; pp. 579–598.
3. Lee, I.M.; Sung, S.G.; Cho, C. Effect of stress state on the unsaturated shear strength of a weathered granite. *Can. Geotech. J.* **2005**, *42*, 624–631. [CrossRef]
4. Vanapalli, S.K.; Pufahl, D.E.; Fredlund, D.G. The effect of soil structure and stress history on the soil-water characteristics of a compacted till. *Géotechnique* **1999**, *49*, 143–159. [CrossRef]
5. Zhou, A.N.; Sheng, D.; Carter, J.P. Modelling the effect of initial density on soil-water characteristic curves. *Géotechnique* **2012**, *62*, 669–680. [CrossRef]
6. Sun, D.A.; Sheng, D.C.; Xu, Y.F. Collapse behaviour of unsaturated compacted soil with different initial densities. *Can. Geotech. J.* **2007**, *44*, 673–686. [CrossRef]
7. Estabragh, A.R.; Javadi, A.A. Critical state for overconsolidated unsaturated silty soil. *Can. Geotech. J.* **2008**, *45*, 408–420. [CrossRef]
8. Gao, Y.; Sun, D.A.; Zhou, A.N. Hydro-mechanical behaviour of unsaturated soil with different specimen preparations. *Can. Geotech. J.* **2016**, *53*, 909–917. [CrossRef]
9. Mendes, J.D.; Toll, G. Influence of initial water content on the mechanical behavior of unsaturated sandy clay soil. *Int. J. Geomech.* **2016**, *16*, D4016005. [CrossRef]
10. Escario, V.; Juca, J.F.T. Strength and Deformation of Partly Saturated Soils. In Proceedings of the 12th International Conference on Soil Mechanics and Foundation Engineering (ICSMFE), Rio de Janeiro, Brazil, 13–18 August 1989; A.A. Balkema: Rotterdam, The Netherlands, 1989; pp. 43–46.
11. Alsherif, N.A.; Mccartney, J.S. Thermal behaviour of unsaturated silt at high suction magnitudes. *Géotechnique* **2015**, *65*, 703–716. [CrossRef]
12. Alsherif, N.A.; Mccartney, J.S. Yielding of silt at high temperature and suction magnitudes. *Geotech. Geol. Eng.* **2016**, *34*, 501–514. [CrossRef]
13. Patil, U.D.; Puppala, A.J.; Hoyos, L.R.; Pedarla, A. Modeling critical-state shear strength behavior of compacted silty sand via suction-controlled triaxial testing. *Eng. Geol.* **2017**, *231*, 21–33. [CrossRef]
14. Sheng, D.C.; Zhou, A.N.; Fredlund, D.G. Shear strength criteria for unsaturated soils. *Geotech. Geol. Eng.* **2011**, *29*, 145–159. [CrossRef]
15. Zhou, A.N.; Huang, R.Q.; Sheng, D.C. Capillary water retention curve and shear strength of unsaturated soils. *Can. Geotech. J.* **2016**, *53*, 974–987. [CrossRef]
16. Mitchell, J.K.; Soga, K. *Fundamentals of Soil Behavior*; Wiley: New York, NY, USA, 2005.

17. Bell, F.G. *Engineering Properties of Soils and Rocks*; Butterworth-Heinemann: Oxford, UK, 1992.
18. Raharjo, H.; Aung, K.K.; Leong, E.C.; Rezay, R.B. Characteristics of residual soils in Singapore as formed by weathering. *Eng. Geol.* **2004**, *73*, 157–169. [CrossRef]
19. Vargas, M. The concept of tropical soils. In Proceedings of the 1st International Conference Geomechanics Tropical Lateritic and Saprolitic Soils, Brasilia, Brazil, 11–14 February 1985.
20. Brand, E.W.; Phillipson, H.B. *Sampling and Testing of Residual Soils: A Review of International Practice*; Scorpion Press: Hong Kong, China, 1985; pp. 1–194.
21. Zhao, J. Engineering properties of the weathered bukit timah granite and residual soils. In Proceedings of the Regional Conference in Geotechnical Engineering, Malacca, Malaysia, 22–24 August 1994.
22. Wu, N.S. Study on classification of granite residual soils. *Rock Soil Mech.* **2006**, *27*, 2299–2304. (In Chinese)
23. Lu, Y.Q.; Wei, C.F.; Cai, G.Q.; Zhao, C.G. Water-holding characteristics of weathered granite soils. *Chin. J. Geotech. Eng.* **2018**, *40*, 96–100. (In Chinese)
24. Bishop, A.W. The principle of effective stress. *Tecknish Ukebl.* **1959**, *106*, 859–863.
25. Fredlund, D.G.; Morgenstern, N.R.; Widger, R.A. The shear strength of unsaturated soils. *Can. Geotech. J.* **1978**, *15*, 313–321. [CrossRef]
26. Alonso, E.E.; Pereira, J.M.; Vaunat, J.; Olivella, S. A microstructurally based effective stress for unsaturated soils. *Géotechnique* **2010**, *62*, 463–465. [CrossRef]
27. Khalili, N.; Khabbaz, M.H. A unique relationship for χ for the determination of the shear strength of unsaturated soils. *Géotechnique* **1998**, *48*, 681–687. [CrossRef]
28. Hillel, D. *Soil and Water: Physical Principles and Processes*; Academic Press: New York, NY, USA; London, UK, 1971.
29. Lu, N.; Likos, W.J. *Unsaturated Soil Mechanics*; Wiley and Sons: New York, NY, USA, 2004.
30. Lu, N.; Khorshidi, M. Mechanisms for soil-water retention and hysteresis at high suction range. *J. Geotech. Geoenviron. Eng.* **2015**, *141*, 04015032. [CrossRef]
31. Baker, R.; Frydman, S. Unsaturated soil mechanics: Critical review of physical foundations. *Eng. Geol.* **2009**, *106*, 26–39. [CrossRef]
32. Lu, N. Generalized soil water retention equation for adsorption and capillarity. *J. Geotech. Geoenviron. Eng.* **2016**, *142*, 04016051. [CrossRef]
33. Gens, A. Soil-environment interactions in geotechnical engineering. *Géotechnique* **2010**, *60*, 3–74. [CrossRef]
34. Konrad, J.M.; Lebeau, M. A capillary-based effective stress Equation for predicting the shear strength of unsaturated soils. *Can. Geotech. J.* **2015**, *52*, 2067–2076. [CrossRef]
35. Tang, L.; Sang, H.; Chen, H.; Sun, Y.; Zhang, L. A quantification model for the structure of clay materials. *J. Appl. Biomater. Funct. Mater.* **2016**, *14*, S29–S34. [CrossRef] [PubMed]
36. Kong, X.A.; Cai, G.Q.; Liu, Z.Z.; Zhao, C.G. Research on tensile-shear coupling strength of unsaturated clays. *Rock Soil Mech.* **2017**, *38*, 9–16. (In Chinese)
37. Liu, E.L.; Nie, Q.; Zhang, J. A new strength criterion for structured soils. *J. Rock Mech. Geotech. Eng.* **2013**, *5*, 156–161. [CrossRef]